ADVANCED MATERIALS INTERFACES
Open Access
www.advmatinterfaces.de

Prospects in Broadening the Application of Planar Solution-Based Distributed Bragg Reflectors

Emilia Palo and Konstantinos S. Daskalakis**

Distributed Bragg reflectors (DBRs) are primarily used in lasers and telecommunications. Liquid film deposition of DBRs holds great promise for expanding their utilization in environmental friendly, low-cost, and large-area applications. In this perspective, this work reviews the progress in solution-based DBR research and evaluates their application in light-emitting devices, photovoltaics and sensing. For these applications, a high refractive index contrast between the alternating layers of a DBR is important for achieving high reflectivity from only a small number of layers. While there is a plethora of solution processes that can produce low-refractive index films, the realization of high-refractive index films is challenging. Recent advances in materials and coating processes have addressed this challenge and novel solution-based DBRs showed remarkable performance which is on par with traditional physical/chemical vapor phase deposition. This work examines what inhibits solution-based DBRs, despite the great progress, to reach the stage of commercial application. In addition, this work found that DBR research is substantially extended beyond photonics, thus by summarizing materials and processes in a single table it aims to provide the necessary information to researchers with diverse backgrounds.

1. Introduction

Since the 1960s, the application spectrum of photonics has been substantially extended from just lasers and telecommunications to lighting, photovoltaics, sensing, imaging and catalysis.[1] To date, it is rather challenging to establish novel photonic solutions as technologically viable—they need to be scalable, cost-effective and use materials that are environmentally friendly and compatible with existing fabrication processes.

Distributed Bragg reflectors (DBRs) are central to photonics research and development. They are dielectric mirrors with a tuneable reflectivity spectrum and have been used extensively in lasers and telecommunications. Because of their simple structure and selective and tuneable reflectivity spectrum, DBRs could be an attractive solution to applications that rely on or benefit from light control. However, high optical-quality DBRs are generally fabricated by physical vapor deposition methods[2,3] which are resource-demanding and complex. DBR's use has been primarily restricted in laser research, thus blocking their widespread use.

Liquid film deposition methods have the potential to circumvent the DBRs' fabrication issues. Recent advances in materials and coating processes have resulted in solution-based DBRs with a remarkable performance which is on par with traditional physical/chemical vapor phase deposition. This has resulted in many interesting DBR applications namely light emission control,[4–6] improving the performance of photovoltaics,[7–10] color-changing sensors[11–13] and recently in catalysis.[14] While DBRs have attractive properties, it is very important to use them only in relevant applications and be cautious when reporting performance gains. For example, controlling solar radiation is a demanding task that DBRs could contribute to, but one needs to also consider that the DBR reflectivity spectrum shifts to blue when increasing the light incidence angle. It is also important to consider whether wet chemical processing of DBRs is a competing or complementary technology to vacuum deposition. We believe that the latter is worth pursuing in the future because it provides easy access to the realization of proofs-of-concept, even when physical vapor deposition equipment is inaccessible.

We note here that the terms solution-based DBRs and solution-processed DBR refer to DBRs made with wet chemistry using material solutions and solution-processing methods. Currently, research in solution-based DBRs is dominated by the use of inorganic nanoparticles, polymer matrices and the combination of these two.[6,14–17] Moreover, recently an interesting approach for the fabrication of DBRs was demonstrated where standing wave interferences were used to pattern photoactive polymers.[18,19] In this perspective, we provide a critical assessment of the recent advancements in solution processing of DBRs and their applications, which is in majority in light-emitting diodes (LEDs), sensors and photovoltaics research. For an extensive review of the field before 2018, the readers are instructed to visit the review article by Lova et al.[1] We found that in many research articles scalability and large area deposition are two of the main motivations for developing solution-based

E. Palo, K. S. Daskalakis
University of Turku
Department of Mechanical and Materials Engineering
Turku FI-20014, Finland
E-mail: emilia.palo@utu.fi; konstantinos.daskalakis@utu.fi

The ORCID identification number(s) for the author(s) of this article can be found under https://doi.org/10.1002/admi.202202206.

DOI: 10.1002/admi.202202206

DBRs. Despite the great progress, there are no examples of true large-area deposition of solution-based DBRs. Instead, research has been extensively focused on developing new soluble material coatings using standard deposition methods such as spin-coating, dip-coating, and doctor blade.

Below we critically assess the respective applications of all the recent articles that state in the title or main text that they have fabricated DBRs. When doing this, we also came across examples that challenge the definition of DBRs—how many alternating pairs are enough to call a coating as DBR? We conclude by evaluating the current state-of-the-art and proposing new research directions. The novelty of solution-based methods is that they enable the utilization of DBRs in low-cost applications. Currently, the main challenge is the discovery of soluble materials and composites that form high-refractive index films that are homogeneous and optically flat.

2. Composition

2.1. DBR Properties

A DBR can be described as a stack of layers with alternating high and low refractive indexes. The fundamentals behind DBR structures can be found in many books about photonics and in some review papers.[1,24,25] In short, a DBR is a superlattice structure, also called 1D photonic crystal, which consists of two alternating films of low and high refractive index, n, materials. Sandwiching layers with large refractive index contrast and minimal absorption in the spectral region of interest results in a highly reflective and spectrally broad DBR stopband (**Figure 1**a,b). The stopband is often referred to as the photonic bandgap in analogy to the electronic bandgap in semiconductors. The high reflectivity in DBRs is the result of the constructive interferences of light reflected from the layer boundaries. The high transparency modes located outside the photonic stopband are called Bragg modes and appear with a period of $2L_{DBR}n_{eff}/\lambda_{vac}$, where L_{DBR} is the thickness, n_{eff} is the effective refractive index of the DBR, and λ_{vac} is the vacuum wavelength of the light. Bragg modes are often overlooked by researchers but for a small number of pairs, we have found that they can accumulate a substantial amount of electromagnetic energy within the DBRs stuck. Every planar interface obeys Snell's law, $n_{ext}\sin\theta_{ext} = n_{int}\sin\theta_{int}$, and DBRs are not an exception. In fact, DBR stopband and Bragg modes shift to shorter wavelengths for increasing the incidence angle of light, as per Snell's law. In addition, when the incidence angle increases, the spectral position of the Bragg mode, stopband, and stopband's spectral width become strongly dependent on the polarization of light. These properties are

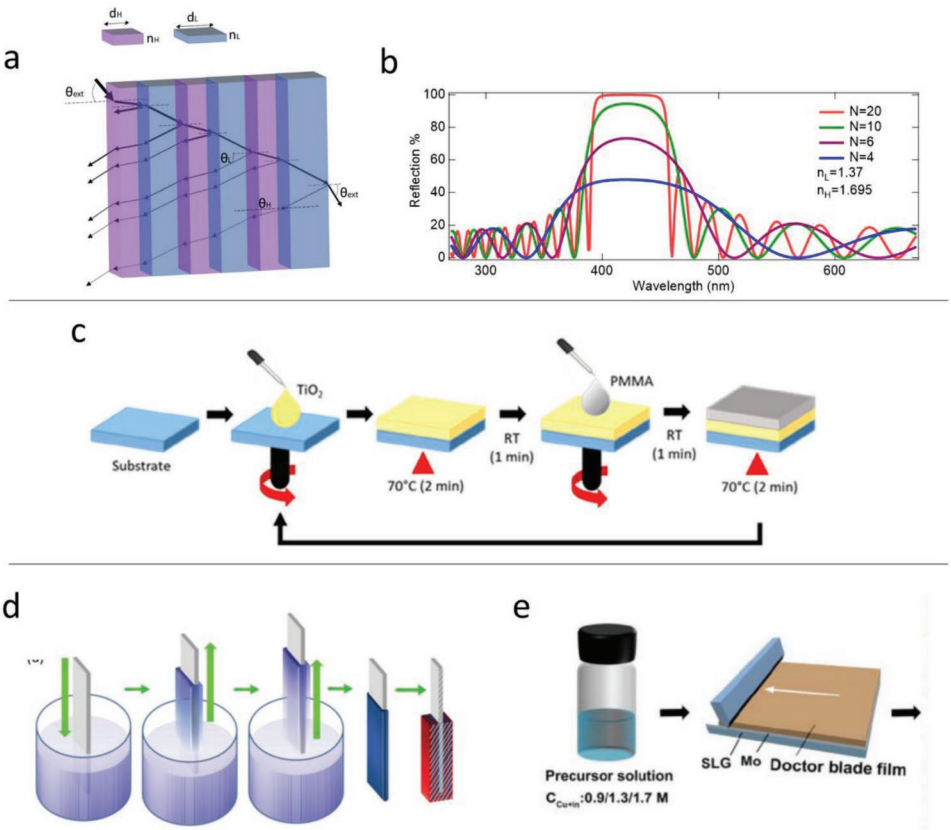

Figure 1. a) Schematic structure of a DBR and b) its reflectivity spectrum at normal incidence for increasing the number of DBR pairs. c) Fabrication schematics of DBRs through spin coating,[20] d) dip coating,[1] and doctor blading[21] methods. Images reproduced with permission.[20] Copyright 2022, John Wiley and Sons/Wiley-VCH, reproduced with permission.[1] Copyright 2018, John Wiley and Sons/Wiley-VCH, reproduced with permission.[21] Copyright 2022, John Wiley and Sons/Wiley-VCH.

rather important when we examine the performance of DBR-based devices but they are often ignored.

Transfer matrix formalism is used to compute the DBR spectrum as a function of the angle for transverse magnetic or transverse electric polarization of light. An example of transfer matrix calculations is visualized in Figure 1a,b and **Figure 2**. For normal incidence, the highest reflectivity and largest spectral width of a stopband are achieved when the optical path for every DBR layer is exactly $\lambda/4 = n_L d_L = n_H d_H$, where the $n_{H/L}$ is the refractive index, $d_{H/L}$ is the optimal thickness and λ is the desired stopband central wavelength. Properly accounting for the correct optical path is essential for maximizing the reflectivity and spectral width of the stopband. The maximum reflectivity is

$$R_{max} = 1 - 4\left(\frac{n_L}{n_H}\right)^N = 1 - 4\left(\frac{n_H - n_L}{n_H}\right)^N \quad (1)$$

while the maximum stopband width is

$$\Delta\lambda = \frac{4\lambda}{\pi}\frac{n_H - n_L}{n_H + n_L} \quad (2)$$

with N representing the number of alternating pairs. Here we see that a large refractive index contrast increases both reflectivity and stopband. It is worth noting that similar to any multilayer structure, the stopband and reflectivity are negatively influenced by inhomogeneity, optical roughness, lattice mismatch and, importantly, absorption in the alternating films. However, these negative effects are more prominent in DBRs consisting of many pairs. This highlights, again, the importance of selecting film combinations with high refractive index contrast, properly accounting for $\lambda/4$ optical path in each layer and minimizing the DBR pairs.

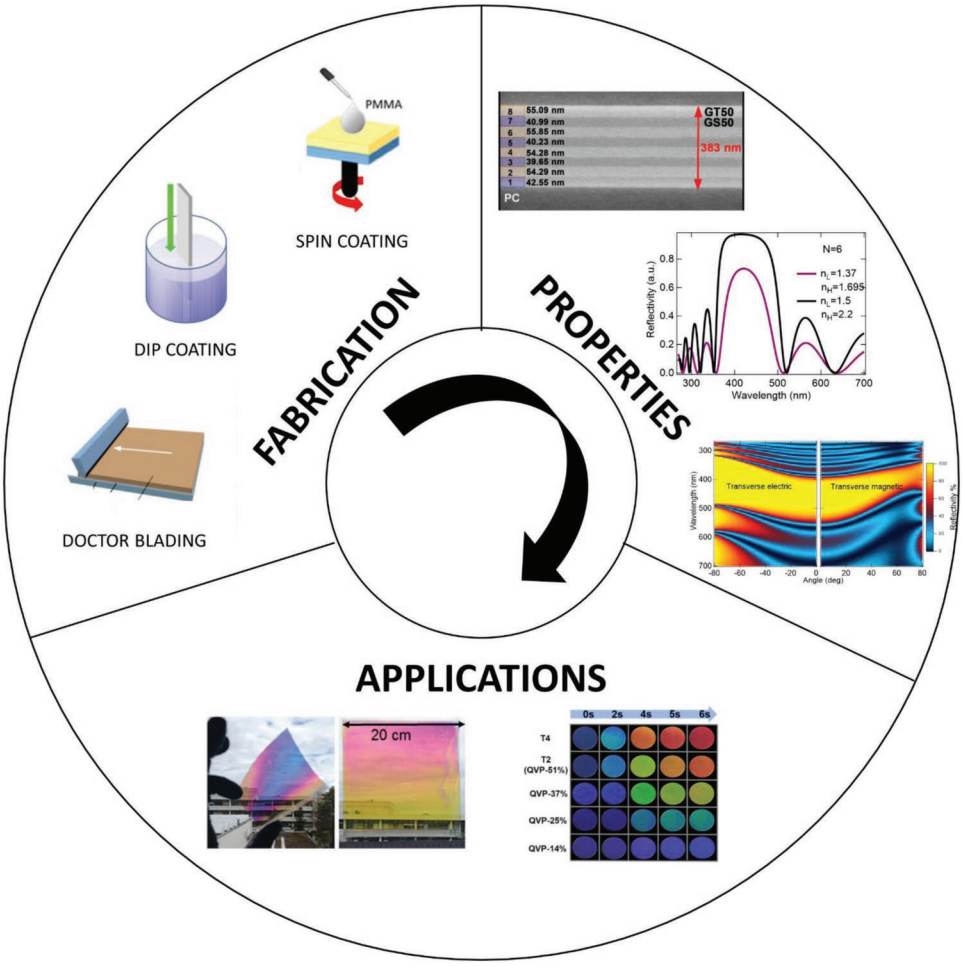

Figure 2. Solution-based DBR fabrication including spin coating, dip coating, and doctor blading with the distinguishable properties of DBRs such as multilayer structure, reflectivity stopband, and angle-dependent reflectivity of a simulated DBR. The use of DBRs in applications such as flexible electronics, large-scale color filters, and sensing by the change of color. Images reproduced with permission.[20] Copyright 2022, John Wiley and Sons/Wiley-VCH, reproduced with permission.[1] Copyright 2018, John Wiley and Sons/Wiley-VCH, reproduced with permission.[21] Copyright 2022, John Wiley and Sons/Wiley-VCH, Zhang et al.[22] Copyright 2021, Royal Society of Chemistry, reproduced with permission.[17] Copyright 2018, John Wiley and Sons/Wiley-VCH, reproduced with permission.[23] Copyright 2021, American Chemical Society.

2.2. State-of-the-Art Materials for DBRs

Inorganic materials have been used extensively in DBRs owing to the availability of composite combinations that lead to large refractive index contrast. The most common DBR combinations are SiO_2/TiO_2 and SiO_2/Ta_2O_5 with refractive index differences (Δn) up to 1.[2,26–28] Other inorganic materials used in DBRs are, for example ZnSe/LiF and HfO_2/Al_2O_3 with a refractive index difference of 0.83 and 0.5, respectively.[29,30] Despite the attractive large refractive index contrast, thin film deposition of the majority of these inorganic materials is commonly realized with vacuum and chemical deposition methods. Similarly, widely used semiconductor DBRs such as GaN, AlGaN, and InGaN are only available through vacuum methods and for that reason they are not discussed further in this perspective.[31–33] As we discussed above, this increases costs and restricts DBR application. This is perhaps extremely challenging, but it would be interesting in the future to attempt thin film deposition of these inorganics with solution-based methods such as liquid phase deposition of oxides.

2.3. Promising Materials for Solution-Based DBRs

A very promising class of materials for the fabrication of DBRs from solution is polymers. They are easy to fabricate through solution-based methods and they can be used as matrices (hosts) for nanoparticles of high refractive index materials like TiO_2. Polymer layers alone often lack a large refractive index difference between layers, thus limiting their use to applications that do not require broad reflectivity stopband or high reflectivity. Polymers with a low refractive index are fluorinated polymers and polydimethylsiloxane (PDMS) with a refractive index of 1.3–1.4[16,34,35] and poly(acrylic acid) (PAA), poly(methyl methacrylate) (PMMA), or poly(vinylalcohol) (PVA) with the refractive index of ≈1.5–1.52.[36–38] There are limited options of polymers with high refractive index. Some examples are poly(*N*-vinylcarbazole) (PVK) which has a refractive index of ≈1.68 and inverse vulcanized polymer S-r-DIT (sulfur-2,5-diisopropylpentiophene-copolymer) with a refractive index of ≈1.8.[37,39] At the current state-of-the-art, the largest reported Δn value in a polymer-based DBR is near 0.35 which is perhaps insufficient for most high-end photonic applications.[40] While there is a plethora of low refractive index polymers, most of them have a refractive index of 1.6 or lower. To overcome this problem and utilize solution-based methods, high-refractive index polymers have been prepared by combining inorganic and organic materials.[14,16] Common approaches are the incorporation of high refractive index inorganic (nano)particles, such as TiO_2, in a polymer matrix or the slow hydrolyzation of Ti-OH in polymer matrices.[16,17,22,41–43] Recently, a refractive index difference of 0.64 at 550 nm was reported in a DBR using hybrid structures of PAA with titanium and silicon.[14]

3. Methods for Fabricating Solution-Based DBRs

The first solution-based DBR was introduced in 1990[1] but they have not found their way to commercial applications, yet. Probably this is because the main application target is the photonics industry which often associates DBRs with applications with high-quality demands. Perhaps, a strategy to overcome this issue is by simply looking at an application that benefits from a solution approach. For example, solution-processed DBR generally have a lower cost because only requires inexpensive equipment, compared with vapor deposition methods. Solution-based methods can cause less damage to the substrate and underlayer that are applied, such as in the application of light-emitting layers. Despite that, during the past decade, various efforts have been made to fabricate high-quality DBRs through solution processing methods. One of the main challenges is the limited selection of large refractive index solution-processed films. In addition, it can sometimes be difficult to find orthogonal solvents meaning that it allows the deposition of several films via a solution process without damage to the underlaid films.

The most common materials and solution-based methods for DBRs are shown in **Table 1**. In the next sections, we take a deeper look into recently developed material combinations and discuss materials and fabrication processes. The specific applications where these materials have been utilized are discussed in Section 4.

3.1. Spin-Coating

In recent years, spin-coating has been used extensively in solution-based DBR fabrication (Table 1). One of the benefits is the easily tuned thickness of the monolayer by only changing the spin speed of the substrate.[44] Due to the centrifugal forces, higher spin speeds produce thinner monolayers. Additional factors that influence the film thickness are the viscosity, precursor concentration, and surface properties of the substrate.[44] Another benefit is that spin-coating is a material-independent deposition method, thus allowing the use of ready-made nanoparticle solutions or sol–gels during the process.[17,45,46] After deposition, annealing, which is the heating of the deposited film, is also commonly used to modify the properties of the spin-coated layer or DBR. Depending on the material solution, annealing can alter the layer thickness, refractive index or both. For instance, the refractive index of Ti-OH/PVA layer can be increased from ≈1.7 to 1.85 by evaporating the solvent at 150 °C after layer deposition.[16] To date, the best approach to achieve a large refractive index contrast between layers with spin coating is to use fluorinated polymer for the low refractive index film, and CuSCN or TiO_2 for the high refractive index film.[4,34,44,47] While spin-coating is an easy-to-use coating method, it is difficult to coat large-area and heavy substrates which are key requirements for the meaningful development of liquid-deposited DBRs.

3.2. Dip-Coating

In addition to spin-coating, dip-coating has been used in solution-based DBRs, though to a much lesser extent (Table 1).[16,43] During the coating process, one can modify the thickness and refractive index of the thin film by tuning the retracting speed

Table 1. Summary of low and high index materials recently used in DBR fabrication with different solution-based methods and their respective stopband spectral region, reflectivity, and the number of layers.

Low index material	High index material	λ_{Bragg}	Reflection at λ_{Bragg}/%	N of layers	Ref.
Spin coating					
Al_2O_3	$PbZr_{0.4}Ti_{0.6}O_3$	450, 600	90, 80	12, 8	[49]
AQ	PVK	405, 600	40, 60	6	[50]
CA	CuSCN	575	90	11	[34]
CA	CuSCN	500, 680, 660	85, 80, 80	9	[4]
CA	HyTiPVA	377, 750	60, 85	21	[41]
CA	poly(S-r-Se-r-DIB)	1000, 1500, 2000	92, 93, 93	22	[51]
CA	PPO	560	55	21	[52]
CA	PS	505, 560, 590	70, 60, 50	41	[5]
CA	PS	530	60	41	[53]
CA	PS	425, 840	60, 80	31	[54]
CA	PS	490	60	31	[11]
CA	PVK	660	60	25	[41]
CA	PVK	480, 550, 640	65, 65,65	11	[34]
CA	PVK	525	80	18	[55]
CA	PVK	600	90	50	[56]
CA	PVK	800	90	50	[6]
CA	ZnO NP in PS	460	60	20	[57]
CA	ZnO NP in PS	500, 750, 1500	40, 40, 40	30	[13]
hPDMS	PDMS/TiO_2	605, 670	90, 90	15	[35]
Hyflon	PVK	450, 900	100, 90	14	[40]
Hyflon	Ti97-Hy	650	80	9	[14]
PAA	IVP:PVK	430	75	21	[39]
PAA	PVK	630,	90	50	[38]
PAA	PVK	725	100	40	[37]
PAA	PVK	630	90	50	[58]
PMMA	PVA-TiO_2	600	30	10	[36]
PMMA-UCNP	TiO_2	1844	90	9	[47]
PMMA	TiO_2-acetylacetone	450, 520, 640	95, 90, 90	54	[20]
PMMA	Ti97-Hy	530	60	7	[14]
PPO	Ti97-Hy	570	50	7	[14]
PSPI	PDMS	540	90	70	[59]
P(VDF-TrFE)	CuSCN	460, 580, 650	95, 90, 90	9	[4]
P(VDF-TrFE)	CuSCN	550	90	9	[34]
P(4VP-*co*-BPA)	P(2VN-*co*-BPA)	420	35	10	[23]
SA	PVK	510	80, 60	21, 13	[60]
SiO_2 NP	ITO NP	500	40	10	[61]
SiO_2	SnO_2	400, 550	20, 12	3	[45]
SiO_2	TiO_2	680	> 90	18	[46]
SiO_2	TiO_2	560, 680, 700, 740	90, 90, 90, 90	5, 7, 5, 5	[44]
SiO_2	TiO_2	420, 520, 650	80, 90, 90	10, 10, 14	[62]
SiO_2	TiO_2	700	70	8	[63]
SiO_2 – GPTMS	TiO_2 – GPTMS	340	70	8	[22]
SiO_2	Zn_2TiO_4	980	> 95	17	[15]
Si97-Hy	Ti97-Hy	580	100	15	[14]
TiO_2 (porous)	TiO_2 (dense)	425	90	13	[64]
Dip coating					
PFP	TiOH/PVA	600	95	21	[16]
SiO_2	SiO_2 _ 30%Ti	510, 1030	60, 50	6	[43]
Doctor blading					
SEBS	ZrO_2-PVA	490	45	20	[12]
SiO_2	PS NP	480, 560. 680	45, 40, 30	7	[48]
SiO_2 ink	TiO_2 ink	470, 530, 680	70, 70, 70	14	[17]

Abbreviations not mentioned earlier in the text; AQ = Aquivion, CA = cellulose acetate, GPTMS = (3-glycidoxypropyl)-trimethoxysilane, Hy = hybrid, ITO = indium tin oxide, NP = nanoparticle, P(2VN-*co*-BPA) = poly(2-vinylnaphthaleneco-benzophenone acrylate), P(4VP-*co*-BPA) = poly(4-vinylpyridine-*co*-benzophenone acrylate), PFP = poly[4,5-difluoro-2,2-bis(trifluoromethyl)-1,3-dioxole-*co*-tetrafluoroethylene], poly(S-r-Se-r-DIB) = poly(sulfur-random-selenium-random-(1,3-diisopropenylbenzene), PPO = Poly(2,6-dimethyl-1,4-phenylene oxide), PS = polystyrene, PSPI = polyisopropene-polystyrene copolymer, P(VDF-TrFE) = poly(vinylidene fluoride-trifluoroethylene), SA = sodium alginate, SEBS = polystyrene-*block*-poly(ethylene-ran-butylene)-*block*-polystyrene, UCNP = upconversion nanoparticle.

and ambient temperature.[43] Depending on the dip-coating retraction speed, different processes are present and affect the film formation, such as capillary forces (slow speed) and solvent evaporation (high speed). In addition, the volatility and concentration of the material solution have a significant effect on the thin film formation. In dip-coating, both sides of the used substrate are being coated simultaneously contrary to spin-coating. Similar to spin-coating, the dip-coated thin layers or DBR stacks can be annealed to modify the composition, crystallinity and thickness of the films. Utilizing inorganic material solutions in the high refractive index layer, dip-coated DBRs have reached reflectivity of up to 95% with 10.5 pairs of TiOH/PVA.[16,43] Because dip-coating relies on gravity and capillary forces, it could also coat irregular surfaces, but no research efforts have been in this direction.

3.3. Doctor Blading

Doctor blading, also known as tape casting, is the only method currently implemented in large area thin film coating because of the easily scalable equipment. In doctor blading, the excess of the coating solution is removed by moving either a blade or roll on the coated surface or moving the substrate below a stationary blade/roll.[17] Control of the film thickness can be achieved by adjusting the concentration of the coating solution, the speed of the moving blade/substrate, or the volume of the deposited solution. Bronnbauer et al. have demonstrated the use of commercial SiO_2 and TiO_2 in "doctor blading" different

sizes of DBRs on both glass and flexible PET foil substrates.[17,42] In addition, other (nano)particles such as zirconium oxide in polystyrene have been used as high refractive index films in DBRs.[12,48] However, apart from the demonstration of Bronnbauer et al. there are no demonstrations with stopband reflectivity larger than 70.[12,48]

4. Applications

4.1. Light-Emitting Devices

Whether optically or electrically driven, a light-emitting device incorporates an emitter (or emitting layer) which largely dictates the performance and optical characteristics of the device. One can tailor the optical properties and improve the performance of a light-emitting device by enhancing the interactions between the emitting layer and its photonic environment; namely by placing the emitter on top of a mirror or inside an optical microcavity. DBRs are excellent mirrors that can also form high optical quality microcavities owning to the ability to reflect only a certain band of wavelengths with minimal absorption losses.[65] In addition, the angular-dependent position of the DBR stopband allows for flexibility in device design and functionality. DBR microcavity architectures can be used to strongly couple the microcavity photon (light) and the exciton of the emitter (matter) for the creation of eigenstates, called polaritons, which can directly improve the characteristics of the emitting material.[66,67] It is important to keep in mind that the optical mode dispersion of DBRs and microcavities has several advantages and disadvantages that purely depend on the desired application. A DBR microcavity can increase the emission (Purcell enhancement) of a light-emitting diode (LED), but its emission will be narrower, will blueshift with increasing the observation angle, and will be concentrated mostly at normal incidence. For example, a DBR microcavity has clear benefits when increasing the emission intensity of a light-emitting device. Still, it has negative implications when it is important to maintain a stable emission color at all angles (Lambertian emission).

Until recently, DBRs were mainly used in laser in which it is essential to have high-quality rather than easy-to-make mirrors. Thus, using the established vacuum deposition methods of inorganic materials was sufficient. The rise of organic LED and lasers has drastically changed this picture. In this case, DBRs made with flexible, sustainable and cheaper methods are favorable. In recent years, solution-based DBRs have been used in all-organic microcavities, organic light-emitting diodes (OLEDs), to modify and enhance the emission of LEDs, and enhance lasing in nanocrystals (**Figure 3**).[4,5,34,37,38]

Lova et al. and Manfredi et al. have demonstrated an all-organic microcavity using DBRs made with PAA/PVK layer structure using J-aggregates of PEH-PBI molecules (phenoxy-functionalized PBI), EuD_4TEA:PS (europium 1,3-diphenyl-1,3-propanedianato complex) composite or CdSe/CdS nanocrystals as emitters.[37,38,56,58] In addition, emitting perovskite structures such as $(EDBE)PbCl_4$ (EDBE = 2,2-(ethylenedioxy)bis(ethylammonium)) with CA/PS and $MAPbI_3$ have been encapsulated with CA/PVK DBRs.[6,53,54] While the all-polymer microcavity had lower quality DBRs due to the typically small dielectric constant difference of polymers, they demonstrated enhanced and directional emission. In addition, they created free-standing plastic VCSEL (vertical cavity surface emitting laser) and induce lasing from the CdSe/CdS nanocrystals, despite the high inhomogeneity in the interfaces. Subsequently, Lova et al. also used an all-polymer DBR which was coupled to a 2D perovskite emitter exhibiting enhanced and directional emission.[5]

Kajii et al. reported a solution-based inorganic/organic DBR using CuSCN/P(VDF-TrFE) multilayers combined with an OLED (Figure 3a).[4,34] Inorganic CuSCN was used as a high refractive index material (n = 1.9), allowing a reasonably large refractive index difference when combined with low refractive index solutions. Using P(VDF-TrFE) instead of CA for the low refractive index component resulted in higher reflectance without increasing the number of layers. Importantly, the DBRs were not damaged during the preparation of the electroluminescent devices.

While solution-based DBRs' Achilles heel is still the low optical quality, they slowly find their niche in light-emitting devices that value cost, sustainability, and production flexibility. Perhaps we will not see any practical applications in lasers, but there might be excellent opportunities in OLEDs. One issue that is often hidden under the rug is the fabrication yield of solution-based DBR light-emitting devices. Many highly-efficient emitting materials require inert conditions when are processed to form devices. But solution-based methods are, in many cases, incompatible with the inert environment and can often chemically react with the emitter. Thus, solving these challenges should be a central point of future research.

Solution processed DBRs key advantage is the ease of fabrication by inexpensive equipment, they could be exploited in

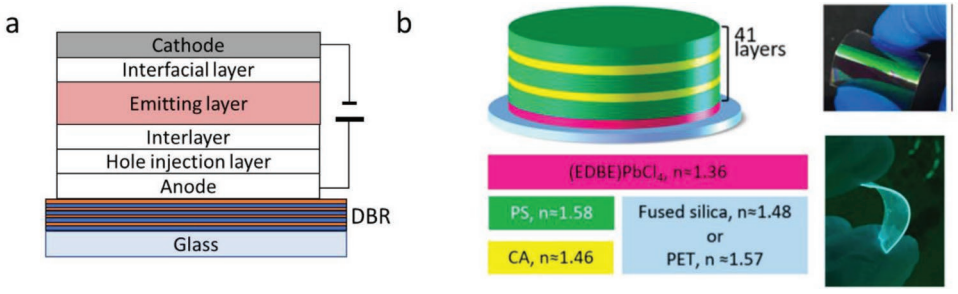

Figure 3. a) An electroluminescent device (LED) structure using DBR to create a microcavity with a metal cathode to enhance their performance. Redrawn from Kajii et al. 2021.[4] b) The structure and visual images of an emitting 2D perovskite where polymer DBR was used to create directional emission. Reproduced with permission from[5] Copyright 2018, American Chemical Society.

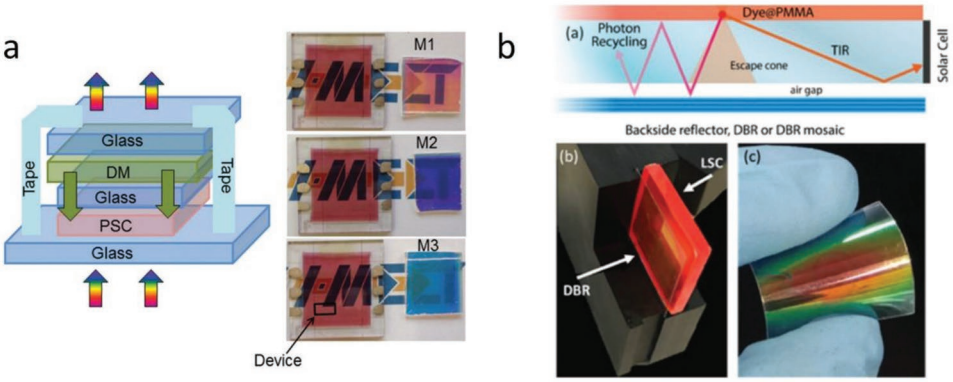

Figure 4. a) Rear-fitted DBR on a polymer solar cell with visual images of the devices. Reproduced with permission[42] Copyright 2015, John Wiley and Sons/Wiley-VCH. b) Schematic of a luminescent solar concentrator with DBR in tandem with a solar cell with visual images of the device and the DBR. Reproduced with permission.[41] Copyright 2019, Royal Society of Chemistry.

prototyping devices for applied and fundamental studies. For example, emerging research in polariton emitting devices, such as OLEDs and lasers, demands optical microcavities to provide the optical confinement for strongly interacting with an exciton. Traditional polaritonic microcavities have been made with physical vapor deposition methods, impeding progress due to many research groups' difficulties to acquire or fabricate polariton samples or prototypes. Therefore, introducing solution-processed microcavities is a promising approach for the rapid advancement of polaritonics research.

4.2. Photovoltaic Devices

Photovoltaic (PV), commonly called solar cells, are optoelectronic devices that convert sunlight into electricity. Perovskite, dye-sensitized, and organic PVs are emerging solar cell technologies but their performance is sensitive to temperature and high energy radiation.

For example, ultraviolet radiation can decompose the dye molecules or increase the photoactivity of TiO_2, which then promotes the formation of destructive radicals in the device structure.[68–70] In both cases the effect on the device performance is detrimental. DBRs could be used to reflect radiation that is not efficiently converted to electrical power, causing unwanted heating to the devices,[10,71–74] while simultaneously beautifying their appearance (colored devices).[20] One overlooked detail in PVs is the growing need for aesthetics, such as a stable color appearance throughout the PV lifetime.[75] DBRs could be one solution to these problems because their color filtering performance is expected to remain uninfluenced by the performance degradation of the PV. Recent examples of utilization of solution-based DBRs in PVs range from fabricating colored devices and aiding in thermal shielding to boosting the luminescent solar concentrators (LSC) and enhancing their output.[41,42,45] In these device structures, the DBR can be situated either over to reflect unwanted radiation or below to enchase absorption of the solar radiation (**Figure 4**a). When the DBR is combined with the LSC, it can also sandwich the emitting material to prevent its emission from escaping through LSC boundaries, enhancing the photovoltaic device performance (Figure 4b). There are also theoretical studies that predict the performance enhancement of silicon-based tandem cells as well as triple-junction solar cells when they are combined with DBRs.[8,47,71] Below we see some more examples.

Safian et al., recently, utilized solution-based DBRs of TiO_2/PMMA and achieved structural coloration of GIGS ($CuIn_xGa_{(1-x)}Se_2$) solar cells.[20] By adjusting the stopbands, blue, green, and red colored solar cells were fabricated with minimal loss in the performance of the GIGS. Similarly, Lee et al. reported blue, yellow and purple perovskite solar cells (PSC) by using a SnO_2/SiO_2 nanoparticle-based DBR structure.[45] However, their color-changing structure consisted only of three layers which might not be sufficient to be classified as a DBR. In their study, the highest photocurrent (15.54 mA cm^{-2}) was achieved with the blue PSC, while the yellow PSC had the highest fill factor (62.33%). Bronnbauer et al., used TiO_2/SiO_2 nanoparticle DBR on a polymer solar cell (100 nm photoactive layer of P3HT:PC_{60} BM (poly(3-hexylthiophene-2,5-diyl) and [6,6]-phenyl-C 60 -butyric acid methyl ester) and reported a photocurrent increase of 24% (increase in J_{sc} from 5.8 to 7.2 mA cm^{-2}).[42] Interestingly, there are no recent experimental studies of solution-based DBRs on state-of-the-art silicon solar cells. This is perhaps due to the already high stability and performance of silicon PVs.

Luminescent solar concentrators (LSCs) are devices that harvest solar radiation from a large surface area and relay its spectrally filter part onto a smaller surface area PV, thus increasing the overall production of electrical power. Portnoi et al. upgraded a dye-doped PDMS LSC by coating its top side with a solution-based DBR consisting of silicone hPDMS and TiO_2 loaded PDMS, and its bottom with a silver mirror.[35] This resulted in increased short circuit current density and power conversion efficiency of the solar cell. Iasilli et al. followed a similar route by coating a fluorescent dye-PMMA LSC with a HyTiPVA/CA (Hydrated titania-poly(vinyl alcohol), cellulose acetate) DBR (Figure 4b).[41] By designing the stopband to be close to the dye emission maxima, they observed an increase in the performance of up to 10%, which was retained even after scaling up the device area by a factor of 4.

In some performance reports, DBR-coated PVs often lack information about their angle-dependent efficiency. As Figure 2

shows, the stopband always shifts towards "blue" wavelengths (higher energy) when the angle of incoming solar (electromagnetic) radiation is increased. In addition, the reflectivity spectrum of a DBR at a large incidence angle is rather different between Transverse Electric (S-polarized) and Transverse Magnetic (P-polarized) light. Considering also that the incidence angle of solar radiation and solar spectrum change dramatically over the daytime, designing a DBR that truly enhances the performance of PVs might be more challenging than it first appears.[76] While in simulation studies, the dispersion of DBR spectrum is usually taken into consideration, most recent experimental publications lack measurements of angle-dependent device performance. Moreover, using DBRs for improving PV performance and aesthetics simultaneously can lead to unwanted effects outside the visible range.[20,77]

Another negative effect of coating PVs with DBRS is the appearance of additional reflective Bragg bands outside the stopband. These, if not suppressed, can restrict radiation that is in the working range of the PV device, reducing its performance. Zheng et al. proposed a theoretical model for suppressing these Bragg reflection bands. However, experimental realization (e-beam evaporation) of the modeled DBR showed that Bragg bands are smaller but still present.[9]

4.3. Sensors

The spectrum of DBRs is very sensitive to changes in the optical path thickness of its layer. This property has been utilized to make sensors with DBRs. This means, that a measured analyte intercalates itself into the DBR layers forcing them to swell, changing the optical path. This creates an observable change in the reflection spectra and can be seen for example as a visual color change (**Figure 5**).[13]

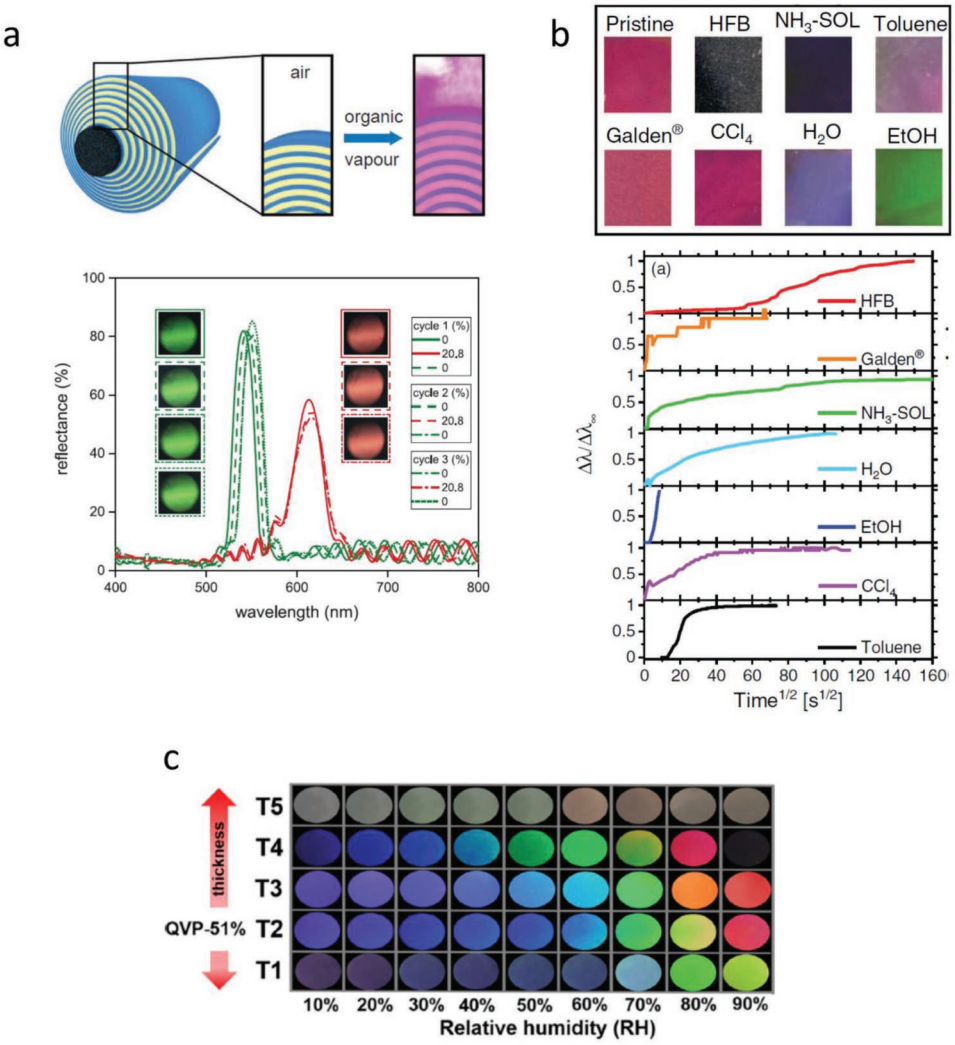

Figure 5. a) Schematic of the sensing through swelling function in an optical fiber DBR and the repeatability of the sensing after swelling cycles. Reproduced with permission.[59] Copyright 2020, John Wiley and Sons. b) Colorimetric and spectral change behavior of a DBR sensor in the presence of different volatile vapor components. Reproduced with permission.[50] Copyright 2021, John Wiley and Sons. c) The spectral response of a DBR-based humidity sensor. Reproduced with permission.[23] Copyright 2021 American Chemical Society.

All-polymer DBRs are currently studied in sensing applications. They can be fabricated rapidly and at a low cost, which is beneficial in applications in pollution surveillance, food degradation sensing or industrial process controls.[23,61] Lately, DBRs have been reported to aid in sensing various volatile organic molecules and humidity, and as detectors for bacterial pollutants and lead from water.[11,12,23,50,57,63,78] Sensing advancements in DBR sensors include the detection of perfluorinated compounds in vapor phase through colorimetric detection using all-polymer DBRs made from Hyflon/PVK multilayers.[40] By comparing DBRs that used different low refractive index layers namely fluorinated Hyflon and cellulose acetate, they found that the detection of perfluorinated compounds required the presence of a fluorinated polymer. This is due to interaction with the fluorinated analyte which then creates a visual change. However, this does not happen with the cellulose acetate, which prevents the swelling in the DBR structure. Moreover, Megahd et al. showed that all-polymer DBR made of AQ/PVK multilayers can be used for sensing a multitude of different chemical species such as ethanol, toluene, water, and HFB (hexafluorobenzene) using visible detection of a color change (Figure 5b).[50] The benefit of DBR structure in this system is that the optical properties of the DBR change differently for each sensed molecule with a different structure offering a possibility to detect multiple analytes with the same system. Similarly, using visible color change as an advantage, Jung et al. demonstrated a humidity sensor from P(4VP-*co*-BPA)/P(2VN-*co*-BPA) DBR where the color response through the visible range could be tuned by either modifying the low refractive index polymer through quaternization or changing its thickness (Figure 5c).[23] Bertucci et al. demonstrated a sol–gel processed hybrid DBR where titanium and silicon alkoxides were combined with poly(allylamine) polymer to produce higher Δn than those all-polymer DBRs.[14] When the low refractive index layer silicon-hybrid was evaluated against all-polymer low refractive index materials, it was shown that the color response of the system could be tuned by the number of DBR layers without compromising the high reflectivity in the structure.

In addition to the abovementioned, Malekovic et al. created a DBR photonic fiber by rolling a double-layer structure (Figure 5a).[59] This type of rolled DBR structure can shift color and optical response due to increased stress along the structure.[79] The ability to add sensing DBR structure to the optical fiber offers a multitude of new applications in textiles and other wearable sensors in which planar structure would not be useful.

Even though polymer DBRs produce a rather narrow and relatively low reflective stop band, they offer ease of fabrication. This has driven studies of sensing in applications, such as food packaging, where disposability of the material and visual detection (such as color change). With the addition of inorganic–organic hybrid materials by Bertucci et al. and the soft fiber detection demonstrated by Malekovic et al., the possibilities in DBR sensing have widened significantly.[14,59] How these new structures fit into large-scale manufacturing, and whether angular dispersion of DBR is a disadvantage remains still a question. Despite these open questions, the possibilities of using DBRs widely in all types of sensing applications seem to be increasing.

5. Conclusion

In summary, we have provided an overview of the recent advances in solution-processed DBRs and their utilization in applications for light emission control, improved photovoltaics performance and color-changing sensors. We have composed a table of different high and low refractive index materials used to create solution-based DBRs and their deposition methods. This table allows for a straightforward overview of the recent methods and materials when new solution-based DBRs are investigated. After examining all the recent literature, it is apparent that the main disadvantage of such DBRs is their low optical quality and inhomogeneity which is a key requirement in applications such as lasers. This stems from the intrinsic challenge of creating solutions of materials and composites that can form high-refractive index films with high homogeneity over large areas. This disadvantage is heavily outweighed by the advantages which are the ability to fabricate them with inexpensive equipment and the potential for large-scale production. The former is essential for prototyping devices, thus rapidly advancing applied and fundamental research, while the latter is important in applications that require low fabrication costs. We found that there has been an increasing interest in developing solution-based DBRs for all types of sensing applications. This, in our opinion, is a very promising direction. Why solution-based DBRs have not yet found their niche in commercial applications is a question that remains open. This is perhaps because a large part of the research has been focused on improving the quality of DBRs which is very challenging and not essential in low-cost applications. Surprisingly, there has been very little effort to demonstrate large-scale deposition which is a key requirement of low-cost applications. Therefore, efforts should be directed toward the development of large-scale DBR by improving the current deposition methods such as doctor-blading or exploring alternative approaches such as inject and spray printing.

Acknowledgements

E.P. and K.S.D. greatly acknowledge the funding from the European Research Council (ERC) Horizon 2020 research and innovation programme (grant agreement No. [948260]) and funding from Business Finland project Turku-R2B-Bragg WOLED with decision number 1951/31/2021, and thank Manish Kumar and Milica Todorović for helpful comments on the manuscript.

Conflict of Interest

The authors declare no conflict of interest.

Keywords

distributed Bragg reflector, microcavities, photovoltaics, sensing, solution methods

Received: October 10, 2022
Revised: November 23, 2022
Published online:

[1] P. Lova, G. Manfredi, D. Comoretto, *Adv. Opt. Mater.* **2018**, *6*, 1800730.
[2] K. S. Daskalakis, F. Freire-Fernández, A. J. Moilanen, S. V. Dijken, P. Törmä, *ACS Photonics* **2019**, *6*, 2655.
[3] K. E. McGhee, A. Putintsev, R. Jayaprakash, K. Georgiou, M. E. O'Kane, R. C. Kilbride, E. J. Cassella, M. Cavazzini, D. A. Sannikov, P. G. Lagoudakis, D. G. Lidzey, *Sci. Rep.* **2021**, *11*, 20879.
[4] H. Kajii, M. Yoshinaga, T. Karaki, M. Morifuji, M. Kondow, *Org. Electron.* **2021**, *88*, 106011.
[5] P. Lova, D. Cortecchia, H. N. S. Krishnamoorthy, P. Giusto, C. Bastianini, A. Bruno, D. Comoretto, C. Soci, *ACS Photonics* **2018**, *5*, 867.
[6] P. Lova, P. Giusto, F. Di Stasio, G. Manfredi, G. M. Paternò, D. Cortecchia, C. Soci, D. Comoretto, *Nanoscale* **2019**, *11*, 8978.
[7] X. Yu, J. Chan, C. Chen, *Nano Energy* **2021**, *88*, 106259.
[8] Y. Jiang, M. J. Keevers, P. Pearce, N. Ekins-Daukes, M. A. Green, *Sol. Energy Mater. Sol. Cells* **2019**, *193*, 259.
[9] L. Zheng, Y. Xuan, *Sol. Energy* **2018**, *173*, 1216.
[10] E. C. Garnett, B. Ehrler, A. Polman, E. Alarcon-Llado, *ACS Photonics* **2021**, *8*, 61.
[11] H. Megahd, P. Lova, D. Comoretto, *Adv. Funct. Mater.* **2021**, *31*, 2009626.
[12] S. Gao, X. Tang, S. Langner, A. Osvet, C. Harreiß, M. K. S. Barr, E. Spiecker, J. Bachmann, C. J. Brabec, K. Forberich, *ACS Appl. Mater. Interfaces* **2018**, *10*, 36398.
[13] P. Lova, G. Manfredi, L. Boarino, A. Comite, M. Laus, M. Patrini, F. Marabelli, C. Soci, D. Comoretto, *ACS Photonics* **2015**, *2*, 537.
[14] S. Bertucci, H. Megahd, A. Dodero, S. Fiorito, F. di Stasio, M. Patrini, D. Comoretto, P. Lova, *ACS Appl. Mater. Interfaces* **2022**, *14*, 19806.
[15] J. Mrázek, L. Spanhel, V. Matějec, I. Bartoň, R. Džunda, V. Puchý, *Opt. Mater.* **2021**, *112*, 110805.
[16] S. Bachevillier, H. K. Yuan, A. Strang, A. Levitsky, G. L. Frey, A. Hafner, D. D. C. Bradley, P. N. Stavrinou, N. Stingelin, *Adv. Funct. Mater.* **2019**, *29*, 1808152.
[17] C. Bronnbauer, A. Riecke, M. Adler, J. Hornich, G. Schunk, C. J. Brabec, K. Forberich, *Adv. Opt. Mater.* **2018**, *6*, 1700518.
[18] B. H. Miller, H. Liu, M. Kolle, *Nat. Mater.* **2022**, *21*, 1014.
[19] S.-L. Li, S.-H. Wang, W.-C. Luo, L.-Q. You, S.-S. Li, L.-J. Chen, *Opt. Express* **2022**, *30*, 33603.
[20] S. Shafian, G. E. Lee, H. Yu, J. Jeong, K. Kim, *Sol. RRL* **2022**, *6*, 2100965.
[21] C. Ma, C. Xiang, X. Liu, B. Li, X. Li, S. Han, Q. Dai, W. Yan, H. Xin, *Solar RRL* **2022**, *6*, 2200150.
[22] J. Zhang, S. Xi, G. Mao, R. Yin, L. Zhu, D. Li, Z. Yao, H. Mi, J. Han, C. Liu, C. Shen, *J. Mater. Chem. C* **2021**, *9*, 4223.
[23] S. H. Jung, H. T. Lee, M. J. Park, B. Lim, B. C. Park, Y. J. Jung, H. Kong, D. H. Hwang, H. Il Lee, J. M. Park, *Macromolecules* **2021**, *54*, 621.
[24] J. D. Joannopoulos, S. G. Johnson, J. N. Winn, R. D. Meade, *Photonic Crystals: Molding the Flow of Light*, Princeton University Press, Princeton, NJ **2011**.
[25] M. Liscidini, L. C. Andreani, *Organic and Hybrid Photonic Crystals*, Springer, Cham **2015**.
[26] B. Gao, J. P. George, J. Beeckman, K. Neyts, *Opt. Express* **2020**, *28*, 12837.
[27] C. T. Prontera, M. Pugliese, R. Giannuzzi, S. Carallo, M. Esposito, G. Gigli, V. Maiorano, *J. Inf. Disp.* **2021**, *22*, 39.
[28] C. Koks, M. P. van Exter, *Opt. Express* **2021**, *29*, 6879.
[29] W. Yu, X. Fu, K. dong, *J. Mater. Sci.: Mater. Electron.* **2021**, *32*, 13409.
[30] T. Sakai, M. Kushimoto, Z. Zhang, N. Sugiyama, L. J. Schowalter, Y. Honda, C. Sasaoka, H. Amano, *Appl. Phys. Lett.* **2020**, *116*, 122101.
[31] C. J. Wu, C. Y. Kuo, C. J. Wang, W. E. Chang, C. L. Tsai, C. F. Lin, J. Han, *ACS Appl. Nano Mater.* **2020**, *3*, 399.
[32] C. J. Wang, Y. Ke, G. Y. Shiu, Y. Y. Chen, Y. sen Lin, H. Chen, C. F. Lin, *Appl. Sci.* **2021**, *11*, 8.
[33] J. R. Pugh, E. G. H. Harbord, A. Sarua, P. S. Fletcher, Y. Tian, T. Wang, M. J. Cryan, *J. Opt.* **2021**, *23*, 035003.
[34] H. Kajii, M. Yoshinaga, T. Karaki, M. Kawata, H. Okui, M. Morifuji, M. Kondow, in *IMFEDK 2019 – International Meeting for Future of Electron Devices Kansai*, IEEE, Piscataway, NJ **2019**, 31–34.
[35] M. Portnoi, T. J. Macdonald, C. Sol, T. S. Robbins, T. Li, J. Schläfer, S. Guldin, I. P. Parkin, I. Papakonstantinou, *Nano Energy* **2020**, *70*, 104507.
[36] L. C. Lohithakshan, V. Geetha, P. Kannan, *Opt. Mater.* **2020**, *110*, 110509.
[37] P. Lova, V. Grande, G. Manfredi, M. Patrini, S. Herbst, F. Würthner, D. Comoretto, *Adv. Opt. Mater.* **2017**, *5*, 1700523.
[38] G. Manfredi, P. Lova, F. Di Stasio, P. Rastogi, R. Krahne, D. Comoretto, *RSC Adv.* **2018**, *8*, 13026.
[39] C. Tavella, P. Lova, M. Marsotto, G. Luciano, M. Patrini, P. Stagnaro, D. Comoretto, *Crystals* **2020**, *10*, 154.
[40] P. Giusto, P. Lova, G. Manfredi, S. Gazzo, P. Srinivasan, S. Radice, D. Comoretto, *ACS Omega* **2018**, *3*, 7517.
[41] G. Iasilli, R. Francischello, P. Lova, S. Silvano, A. Surace, G. Pesce, M. Alloisio, M. Patrini, M. Shimizu, D. Comoretto, A. Pucci, *Mater. Chem. Front.* **2019**, *3*, 429.
[42] C. Bronnbauer, J. Hornich, N. Gasparini, F. Guo, B. Hartmeier, N. A. Luechinger, C. Pflaum, C. J. Brabec, K. Forberich, *Adv. Opt. Mater.* **2015**, *3*, 1424.
[43] I. Barton, V. Matejec, J. Mrazek, L. Predoana, M. Zaharescu, *Opt. Mater.* **2018**, *77*, 187.
[44] V. Yepuri, R. S. Dubey, B. Kumar, *Sci. Rep.* **2020**, *10*, 15930.
[45] J. H. Lee, Y. Song, K. Jung, M. J. Lee, *Mater. Lett.* **2021**, *282*, 128828.
[46] M. Malekovic, E. Bermúdez-Urenã, U. Steiner, B. D. Wilts, *APL Photonics* **2021**, *6*, 026104.
[47] C. L. M. Hofmann, S. Fischer, E. H. Eriksen, B. Bläsi, C. Reitz, D. Yazicioglu, I. A. Howard, B. S. Richards, J. C. Goldschmidt, *Nat. Commun.* **2021**, *12*, 104.
[48] B. Q. Kim, Y. Qiang, K. T. Turner, S. Q. Choi, D. Lee, *Adv. Mater. Interfaces* **2021**, *8*, 2001421.
[49] S. Li, W. Zhao, Y. Sun, N. Dai, G. Hu, *AIP Adv.* **2020**, *10*, 055224.
[50] H. Megahd, C. Oldani, S. Radice, A. Lanfranchi, M. Patrini, P. Lova, D. Comoretto, *Adv. Opt. Mater.* **2021**, *9*, 2002006.
[51] T. S. Kleine, L. R. Diaz, K. M. Konopka, L. E. Anderson, N. G. Pavlopolous, N. P. Lyons, E. T. Kim, Y. Kim, R. S. Glass, K. Char, R. A. Norwood, J. Pyun, *ACS Macro Lett.* **2018**, *7*, 875.
[52] P. Lova, C. Bastianini, P. Giusto, M. Patrini, P. Rizzo, G. Guerra, M. Iodice, C. Soci, D. Comoretto, *ACS Appl. Mater. Interfaces* **2016**, *8*, 31941.
[53] P. Lova, D. Cortecchia, C. Soci, *Appl. Sci.* **2019**, *9*, 5203.
[54] P. Lova, G. Manfredi, C. Bastianini, C. Mennucci, F. B. De Mongeot, A. Servida, D. Comoretto, *ACS Appl. Mater. Interfaces* **2019**, *11*, 16872.
[55] M. Athanasiou, P. Papagiorgis, A. Manoli, C. Bernasconi, M. I. Bodnarchuk, M. V. Kovalenko, G. Itskos, *ACS Photonics* **2021**, *8*, 2120.
[56] G. Manfredi, P. Lova, F. Di Stasio, R. Krahne, D. Comoretto, *ACS Photonics* **2017**, *4*, 1761.
[57] P. Lova, *Polymers* **2018**, *10*, 1161.
[58] P. Lova, M. Olivieri, A. Surace, G. Topcu, M. Emirdag-eanes, M. M. Demir, D. Comoretto, *Crystals* **2020**, *10*, 287.
[59] M. Malekovic, M. Urann, U. Steiner, B. D. Wilts, M. Kolle, *Adv. Opt. Mater.* **2020**, *8*, 2000165.
[60] A. Dodero, P. Lova, S. Vicini, M. Castellano, D. Comoretto, *Chemosensors* **2020**, *8*, 37.
[61] G. M. Paternò, C. Iseppon, A. D'Altri, C. Fasanotti, G. Merati, M. Randi, A. Desii, E. A. A. Pogna, D. Viola, G. Cerullo, F. Scotognella, I. Kriegel, *Sci. Rep.* **2018**, *8*, 3517.
[62] R. S. Dubey, V. Ganesan, *Superlattices Microstruct.* **2018**, *122*, 228.

[63] M. C. Sansierra, J. Morrone, F. Cornacchiulo, M. C. Fuertes, P. C. Angelomé, *ChemNanoMat* **2019**, *5*, 1289.
[64] X. Hu, Z. Zhang, X. Chen, M. Luo, *Nanotechnology* **2020**, *31*, 135209.
[65] A. J. C. Kuehne, M. C. Gather, *Chem. Rev.* **2016**, *116*, 12823.
[66] D. Sanvitto, S. Kéna-Cohen, *Nat. Mater.* **2016**, *15*, 1061.
[67] F. J. Garcia-Vidal, C. Ciuti, T. W. Ebbesen, *Science* **2021**, *373*, 1979.
[68] T. Leijtens, G. E. Eperon, S. Pathak, A. Abate, M. M. Lee, H. J. Snaith, *Nat. Commun.* **2013**, *4*, 2885.
[69] J. Ji, X. Liu, H. Jiang, M. Duan, B. Liu, H. Huang, D. Wei, Y. Li, M. Li, *iScience* **2020**, *23*, 101013.
[70] A. Poskela, K. Miettunen, A. Tiihonen, P. D. Lund, *Energy Sci. Eng.* **2021**, *9*, 19.
[71] G. Perrakis, A. C. Tasolamprou, G. Kenanakis, E. N. Economou, S. Tzortzakis, M. Kafesaki, *Opt. Express* **2020**, *28*, 18548.
[72] C. Chen, S. Zheng, H. Song, *Chem. Soc. Rev.* **2021**, *50*, 7250.
[73] B. M. Cote, I. M. Slauch, M. G. Deceglie, T. J. Silverman, V. E. Ferry, *ACS Appl. Energy Mater.* **2021**, *4*, 5397.
[74] I. M. Slauch, M. G. Deceglie, T. J. Silverman, V. E. Ferry, *ACS Appl. Energy Mater.* **2019**, *2*, 3614.
[75] Q. Bao, T. Honda, S. El Ferik, M. M. Shaukat, M. C. Yang, *Renewable Energy* **2017**, *113*, 1569.
[76] O. Dupré, B. Niesen, S. De Wolf, C. Ballif, *J. Phys. Chem. Lett.* **2018**, *9*, 446.
[77] A. Ghosh, *Sol. Energy* **2022**, *237*, 213.
[78] G. M. Paternò, G. Manfredi, F. Scotognella, G. Lanzani, *APL Photonics* **2020**, *5*, 080901.
[79] M. Kolle, A. Lethbridge, M. Kraysing, J. J. Baumberg, J. Aizenberg, P. Vukusic, *Adv. Mater.* **2013**, *25*, 2239.

Emilia Palo is a postdoctoral researcher at the Department of Mechanical and Materials Engineering at the University of Turku. She obtained her Ph.D. from the Department of Chemistry at the University of Turku in 2019. Her research interests are focused on developing new and sustainable ways of using optical thin films and/or photoactive materials in different applications.

Konstantinos S. Daskalakis is currently an Assistant Professor and ERC starting grant holder at the Department of Mechanical and Materials Engineering at the University of Turku. He obtained his Ph.D. from Imperial College London in 2014 and received the Marie Skłodowska-Curie Research Fellowship in 2017 to continue his research at Aalto University. His group of Luminous Materials and Devices aims to utilize materials science, photonics and solid-state physics to improve light-emitting devices and to engineer novel materials for lighting applications.